DYNA
http://dyna.medellin.unal.edu.co/

UNIVERSIDAD NACIONAL DE COLOMBIA

Analysis of potential waste heat recovery from a stenter in a textile plant

Ricardo Mazo-Restrepo, Pedro Alvarado & Karen Cacua

Facultad de Ingenierías, Grupo de Investigación Materiales Avanzados y Energía, Instituto Tecnológico Metropolitano, Medellín, Colombia. ricardomazo190223@correo.itm.edu.co, pedroalvarado@itm.edu.co, karencacua@itm.edu.co

Received: February 3rd, 2021. Received in revised form: April 20th, 2021. Accepted: May 4th, 2021.

Abstract
The textile sector, an important economic driving force in Antioquia, Colombia, uses great quantities of thermal energy mainly produced by coal combustion, which holds enormous potential for recovery. One of the most common processes in a textile plant is heat setting, which uses a significant amount of thermal energy to adjust the properties of fabrics, such as shrinking, stiffness, pull strength, width, and stretching. In this study, we calculate the mass and energy balances of a stenter and propose a system to recover the energy available in its exhaust gases. The energy recovery potential in this heat setting process is 800.97 kW, which represents 87.2% of the total input energy. Additionally, we evaluate different heat exchangers to recover the available heat and present criteria to select them. Finally, thermosyphons, whose thermal efficiency was theoretically determined here, offer a promising alternative for heat recovery from actual stenters.

Keywords: stenter; heat setting; textile plant; waste heat recovery; heat pipes; thermal energy.

Análisis del potencial de recuperación de calor residual de una termofijadora en una planta textil

Resumen
El sector textil, un importante motor económico de Antioquia, Colombia, usa grandes cantidades de energía térmica, principalmente producida por la combustión de carbón y tiene un enorme potencial de recuperación. Uno de los procesos en una planta textil es el termofijado, el cual usa una cantidad significativa de energía térmica para ajustar las propiedades de la tela, tales como encogimiento, rigidez, fuerza de tracción, ancho y estiramiento. En este estudio, se realizó el balance de masa y energía de una termofijadora y se propuso un sistema para recuperar la energía en sus gases de escape. El potencial de recuperación de energía en el proceso de termofijado fue de 800,97 kW, representando 87,2% de la energía total de entrada. Adicionalmente, se evaluaron diferentes opciones de intercambiadores de calor. Finalmente, los termosifones, cuya eficiencia térmica se determinó teóricamente, ofrecen una alternativa viable para la recuperación de calor de las termofijadoras.

Palabras Clave: termofijadora textil; termofijado; planta textil; recuperación de calor residual; termosifones; energía térmica.

Nomenclature

$\dot{m}_{waterEC1}$ = Water mass flow inlet to the air circulation chamber 1 [kg/s]
$\dot{m}_{Fin}$ = Fabric mass flow inlet to stenter machine [kg/s]
$\dot{m}_{AirRTEC1}$= Air mass flow inlet to circulation chamber 1 [kg/s]
W_{FAE} = Fans and extractors power [kW]
$\dot{m}_{AirLE1}$ = Air mass flow outlet from the extraction duct 1 [kg/s]
$\dot{m}_{WaterLE1}$ = Water mass flow outlet from the extraction duct 1 [kg/s]
$\dot{m}_{AirLE2}$ = Air mass flow outlet from the extraction duct 2 [kg/s]
$\dot{m}_{WaterLE2}$ = Water mass flow outlet from the extraction duct 2 [kg/s]
$\dot{m}_{WaterOC7}$ = Water in the fabric outlet from the air circulation chamber 7 [kg/s]
$\dot{m}_{Foutlet}$ = Fabric mass flow outlet from the stenter machine [kg/s]
$\dot{m}_{AirRTEC7}$ = Air mass flow inlet to the circulation chamber 7 [kg/s]
$\dot{m}_{OILin}$= Hot oil mass flow inlet to [kg/s]
$\dot{m}_{OILoutlet}$ = Hot oil mass flow outlet the heat exchangers set [kg/s]
$\dot{m}_{WaterEvp}$ = Evaporated water in the stenter machine [kg/s]
$\dot{m}_{WaterERTAC1}$ = Water mass flow inlet to air circulation chamber 1 [kg/s]

How to cite: Mazo-Restrepo, R., Alvarado, P. and Cacua, K., Analysis of potential waste heat recovery from a stenter in a textile plant.. DYNA, 88(217), pp. 292-302, April - June, 2021.

$\dot{m}_{WaterERTAC7}$ = Water mass flow inlet to air circulation chamber 7 [kg/s]
TFM = Total fabric meters [m]
WER= Weight of each roll [kg]
V = Fabric speed [m/min]
CP_{OilIN} = Specific heat of hot oil (inlet) [kJ/kg°C]
T_{OilIN} = Oil inlet temperature [°C].
CP_{FIN} = Specific heat of fabric [kJ / kg ° C]
T_{FIN} = Fabric inlet temperature [°C]
$h_{WaterEC1}$ = Enthalpy of water inlet to the circulation chamber 1 [kJ/kg]
$h_{AirRTEC1}$ = Enthalpy of air inlet to circulation chamber 1 [kJ/kg]
$h_{AirRTEC7}$ = Enthalpy of air inlet to circulation chamber 7 [kJ/kg]
$h_{WaterLC7}$ = Enthalpy of water outlet in the fabric in the circulation chamber 7 [kJ/kg]
CP_{OilO} = Specific heat of hot oil (outlet) [kJ/kg°C]
T_{OilO} = Hot oil temperature outlet [°C].
CP_{FO} = Specific heat of the fabric (outlet) [kJ/kg°C]
T_{FO} = Fabric outlet temperature [°C]
h_{AirLE1} = Air enthalpy from extractor 1 [kJ/kg]
h_{AirLE2} = Air enthalpy outlet from extractor 2 [kJ/kg]
h_{Evp} = Latent heat of water [kJ/kg]
$HrelRT$ = Relative humidity at room temperature

1. Introduction

Nowadays, the high demand for energy and the effects of climate change have motivated a search for new alternatives that improve the efficiency of industrial processes. In particular, waste heat recovery has been widely implemented to improve energy efficiency. It has been estimated that between 20% and 50% of the energy used in the industrial sector is wasted as heat in the form of hot exhaust gases, cooling water, and heat losses from the surfaces of hot equipment and heated products [1]. The textile sector presents great opportunities to increase its energy efficiency by using the waste heat from equipment that offer high energy availability, such as boilers, natural gas generators, waste water form dyeing, and stenters [1–4].

In the textile sector, stenter machines can consume up to 30% of the total thermal energy that is used, and potential energy savings in this process oscillate between 20% and 70% [5]. Heat setting, part of the finishing process applied to fabrics, aims to provide the fabric with dimensional stability by thermally fixing the fibers. In stenter machines, most power is used to evaporate water in the fabric and heat air [6]. The power consumption of this process depends on the specific operation and fuel, but it varies between 2.5–7.5 GJ/ton in the drying and 4.0–9.0 GJ/ton in the heat setting stages [6]. Nevertheless, when optimized, such consumption can be as low as 3.5–4.5 MJ/ton of processed fabric [5].

In general, to increase the energy efficiency of heat setting, heat exchangers are implemented to recover the waste energy in the gases it produces. Some of the most common types of heat recovery are recirculation, tube heat exchangers, plate heat exchangers, thermal wheels, heat pipes, run-round coils, and direct contact coolers [7]. The selection of the type of heat exchanger depends on different criteria such as effectiveness, fouling factor, cost, and payback period. Furthermore, such selection and energy recovery level also depend on the specific operation conditions of the equipment that can provide waste heat [8].

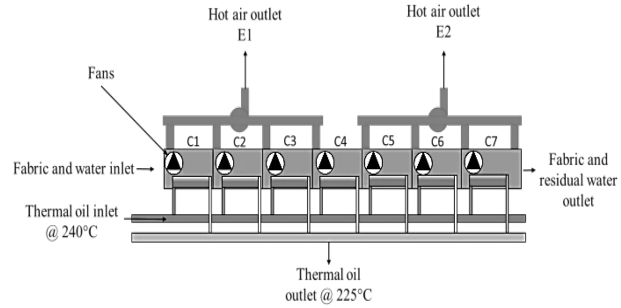

Figure 1. General scheme of the heated chambers in the stenter, the outlet ducts of Chambers 1–4 are connected by Extractor fan 1 (E1). Likewise, the outlet ducts of Chambers 5–7 are connected by Extractor fan 2 (E2). Each chamber is heated using a heat exchanger through which hot thermal oil is circulated.
Source: the authors

Therefore, increasing the energy efficiency in industrial processes by heat recovery is an opportunity to obtain economic and environmental benefits. In this study, we calculated the mass and energy balances in an actual heat setting process in a company in textile sector in Antioquia and determined the amount of thermal energy that could be recovered. Finally, we applied specific criteria to select one of the most commonly used heat recovery technologies for this purpose and determined the thermal energy recovery potential using such technology.

2. Methodology

In this article, we studied a KRANZ stenter which is currently in operation. It has seven air circulation chamber and two hot gas extractor fans. The mass and energy balances were calculated only in the heated chambers because that is where the heat transfer occurs in order to dry and heat set the fabric. Fig. 1 presents a scheme of the seven heated chambers.

2.1 Mass and energy balance of the stenter

This mass and energy balance and the assumptions made here are based on previous studies [9–11]. We used the scheme in Fig. 2, which shows each one of the mass and energy inlets and outlets found in the stenter.

Hypotheses for the mass and energy balance:

- There is no heat transfer between the stenter walls and the environment. This assumption is based on the fact there is glass fiber insulation (10 cm thick), and the temperature of the wall measured at 70 random points was 43±2 °C.
- The heat setting process is carried out in stationary conditions.
- The composition of the outlet gases of the stenter is assumed to be similar to that of air.
- Regarding the sign convention, the heat transfers to the system and the work transfer are positive.

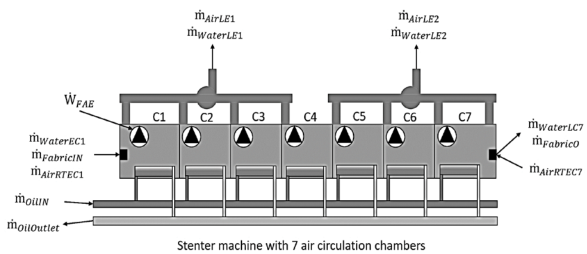

Figure 2. Scheme for mass and energy balance.
Source: the authors

2.1.1 Mass balance

Fig. 2 presents the scheme for the mass balance of the system, which was established considering different fluids and materials: hot oil, air used to dry/heat set the fabric, water contained in the air, and fabric.

We used the following equations in the mass balance of the stenter:

Mass balance of the fabric (1):

$$\dot{m}_{Fin} = \dot{m}_{Foutlet} = \dot{m}_{Fabric} \qquad \textbf{(1)}$$

Mass balance of the oil (2):

$$\dot{m}_{OilIN} = \dot{m}_{Oiloutlet} = \dot{m}_{Oil} \qquad (2)$$

Eqs. (3)–(4) present the mass balance of air. Bearing in mind that Extractor fan 1 is connected to heated Chambers 1–4 and Extractor fan 2 is connected to Chambers 5–7, we have:

$$\dot{m}_{AirRTEC1} = \dot{m}_{AirLE1} - \dot{m}_{WaterEvp} \qquad (3)$$

$$\dot{m}_{AirRTEC7} = \dot{m}_{AirLE2} \qquad (4)$$

Eqs. (5)–(8) present the mass balance of water. In general, when polyester/cotton is processed, the fabric is dried in the first three heated chambers and heat set in the other four.

$$\dot{m}_{WaterEC1} - \dot{m}_{WaterLC7} = \dot{m}_{WaterEvp} \qquad (5)$$

$$\dot{m}_{WaterEvp} + \dot{m}_{WaterERTAC1} = \dot{m}_{WaterLE1} \qquad (6)$$

$$\dot{m}_{WaterERTAC1} = (\dot{m}_{AirRTEC1} \times H_{relRT}) \qquad (7)$$

$$\begin{aligned}\dot{m}_{WaterERTAC7} &= (\dot{m}_{AirRTEC7} \times H_{relRT}) \\ &= \dot{m}_{WaterLE2}\end{aligned} \qquad (8)$$

The parameters required for the mass and energy balance were experimentally obtained. The mass flow rate of the fabric was obtained with the mass and the time the fabric is exposed in the stenter.

The stenter was started, but the fabric was kept in place for us to measure the temperature in each area before entering the heated chambers and at the outlet of such chambers. We used a RAYTEK ST20 PRO infrared thermometer with a range between -32 and 400°C ± 1°C and an emissivity of 0.95, which is adequate to measure fabric temperatures [12].

The fabric yield, considering the weight and length of each roll of fabric, was calculated using Eq. (9).

$$Yield = \left[\frac{TFM}{WER}\right]\left[\frac{m}{kg}\right] \qquad (9)$$

where, with the velocity of the fabric and the yield, the mass flow rate was calculated with Eq. (10).

$$\dot{m}_{fabric} = \left[\frac{V}{Yi\ eld}\right]\left[\frac{kg}{min}\right] \qquad (10)$$

2.1.2 Mass flow rate of air and exhaust air temperatures

The mass flow rate of the hot air that is released into the atmosphere was calculated with the volumetric flow rate and density. The volumetric flow rate was measured using a Pitot-type TESTO 485-4 differential pressure meter, which is also equipped with a Type K temperature probe with a measurement range between -60 and 400°C. Such rate was measured considering the requirements described in [13].

2.1.3 Mass flow rate of the water that enters along with air into the stenter

The moisture of the air that enters the stenter was determined using the psychrometric properties of air and using an online psychrometric calculator that enables users to make corrections for altitude [14].

2.1.4 Mass flow rate of evaporated water

To determine the mass flow rate of water, we measured the fabric moisture before and after the process by taking representative pieces of fabric and analyzing them in a Precisa XM60-HR moisture analyzer. The mass flow rate of evaporated water was calculated using the difference between the inlet and outlet fabric moisture.

2.2 Energy balance

To calculate the energy balance, we took into consideration the mass flow rates of the fluids in the process and the fabric, as well as the power of the fans. Eq. (11) presents the energy balance we implemented.

$$\begin{aligned}\dot{m}_{OIL}\ (CP_{OilIN} \times T_{OilIN}) + \dot{m}_{Fabric}\ (CP_{FIN} \times T_{FIN}) \\ + (\dot{m}_{WaterEC1} \times h_{WaterEC1}) \\ + (\dot{m}_{WaterERTAC1} \times h_{WaterEC1}) \\ + (\dot{m}_{WaterERTAC7} \times h_{WaterEC7}) \\ + (\dot{m}_{AirRTEC1} \times h_{AirRTEC1}) \\ + (\dot{m}_{AirRTEC7} \times h_{AirRTEC7}) \\ + \dot{W}_{FAE} \\ = \dot{m}_{OIL}\ (CP_{OILO} \times T_{OILO}) \\ + (\dot{m}_{WaterOC7} \times h_{WaterLC7}) \\ + \dot{m}_{Fabric} (CP_{FO} \times T_{FO}) \\ + (\dot{m}_{AirLE1} \times h_{AirLE1}) \\ + (\dot{m}_{AirLE2} \times h_{AirLE2}) \\ + \Big((\dot{m}_{WaterEvp} \\ + \dot{m}_{WaterLE1}) h_{Evp}\Big) \\ + (\dot{m}_{WaterLE2} \times h_{Evp})\end{aligned} \quad (11)$$

The properties of the fluids and the fabric were determined using tables of thermodynamic properties [15]. The instantaneous power of the fans was measured using a Fluke 435 power quality analyzer.

2.3 Selecting a heat exchanger to recover heat from the stenter

Since different types of heat exchangers can be used to recover heat in the textile industry, we defined specific selection criteria to find the best alternative (see). Such criteria, taken and adapted from [7], were assigned values that depend on the system requirements.

Once we applied the values of the selection criteria to each exchanger, we obtained the results in Table 2. Additionally, considering that higher values represent better options, Table 3 presents a more detailed analysis of each type of exchanger that can be used to recover waste heat from the stenter.

2.4 Methodology to design the heat exchanger

Based on the methodological analysis described above, heat pipes are a viable solution to recover heat in this case. The exchanger was designed using an iterative process to find the best arrangement of the thermosyphons. This process was completed following the decision-making map in Fig. 3. The equations to find the value of each variable in this map were taken from [15–19]. The constraints to define the final geometry of the exchanger included:

Table 1.
Selection criteria and assigned values.

Cost	
Low	10.00
Moderate	7.50
Moderate-high	5.00
High	2.50
Gas-side fouling	
Yes	0.00
No	10.00
Contamination of fresh air (Effect on final product)	
Yes	0.00
No	10.00
Access for maintenance	
Yes	10.00
No	0.00
Efficiency	
100%	10.00
90%	9.00
80%	8.00
70%	7.00
60%	6.00
50%	5.00
40%	4.00
30%	3.00
20%	2.00
10%	1.00
0%	0.00
Additional equipment besides fans (Negative impact on the total recovered energy, e.g., pumps and reducers)	
Yes	0.00
No	10.00

Source: authors' elaboration

- A gas outlet temperature of 100°C ± 2°C
- A maximum bank width of 1300 mm (The ducts of the stenter are 750 mm. This constraint seeks to avoid abrupt transitions at the inlet, which can result in the fluid only going through the middle and not coming into contact with the thermosyphons located on the sides.)

Table 2.
Application of selection criteria to several types of heat recovery.

	Type of heat recovery							
Selection criterion	**Recirculation**	**Shell and tube heat exchanger**	**Plate heat exchanger**	**Therma l wheel**	**Heat pipe**	**Run-round coils**	**Direct contact cooler**	**Finned concentric**
Cost	10.00	5.00	7.50	5.00	5.00	5.00	10.00	5.00
Gas-side fouling	10.00	0.00	0.00	0.00	0.00	0.00	0.00	0.00
Contamination of fresh air	0.00	10.00	10.00	2.00	10.00	10.00	10.00	10.00
Access for maintenance	10.00	0.00	0.00	10.00	10.00	10.00	10.00	10.00
Efficiency	3.00	6.00	7.00	8.00	6.00	5.50	9.50	7.00
Additional equipment or moving parts	10.00	10.00	10.00	0.00	10.00	0.00	10.00	0.00
Total score	**43.00**	**31.00**	**34.50**	**25.00**	**41.00**	**30.50**	**49.50**	**32.00**

Source: authors' elaboration

Table 3.
Technical analysis of heat exchangers applicable to heat recovery from stenters.

Type of heat recovery	Score	Comments
Direct contact cooler	49.50	Although this exchanger offers the highest efficiency in this group, it would require liquid to transfer heat. However, such liquid is highly likely to retain contaminants in the flow of gas coming from the stenter. Additionally, if the recovered heat is to be used in the same stenter, another liquid/gas exchanger and auxiliary equipment, such as pumps and valves, are necessary.
Reticulation	43.00	The problem with this exchanger is that it is highly likely to contaminate the final product (fabric) because the gases may contain fibers, dust, or dyestuff residue from the dyeing process.
Heat pipe	41.00	This feasible solution to recover heat requires a new fan to move the fresh air to be heated. Nevertheless, it is not difficult to manufacture, which is why it can be easily replicated.
Plate heat exchanger	34.50	The main drawback of this type of exchangers is that the plates provide no access for cleaning and maintenance, due to which they may lose efficiency over time caused by fouling. Additionally, manufacturing them is not a simple process and they represent a high cost.
Finned concentric	32.00	Although this is an affordable option that can reach high efficiencies, it requires adding equipment such as pumps (which reduces the final recovered power), valves, and a liquid/gas exchanger to inject the recovered heat back into the stenter. This system is very similar to run-round coils.
Shell and tube heat exchanger	31.00	In spite of being one of the most widely known types of exchanger, it suffers from the same limitations as plate heat exchangers.
Run-round coils and thermal wheel	30.50 and 25.00, respectively	The main limitation of these two types of exchanger is that they need additional equipment, which may reduce the final recovered power. Additionally, thermal wheels can pollute fresh air, are more expensive to manufacture, are not easy to replicate, and require regular maintenance.

Source: authors' elaboration

2.4.1 Working fluid and thermosyphon material

The working fluid and the material of the thermosyphons were selected considering the temperature range of the gases and the recommendations in [20].

2.4.2 Hydraulic design of the heat recovery system

The pressure drop was calculated using Eq. (11) [15]

$$\Delta P = N_L f\ X \left(\frac{\rho V_{max}^2}{2}\right) \tag{11}$$

The electric power required to move the fluids through the exchanger depends on the pressure drop (ΔP), and it was calculated with Eq. (12)

$$\dot{W}_{Fan} = \frac{\dot{m}.\Delta P}{\rho}\ [W] \tag{12}$$

3. Results

3.1 Mass balance

Table 4 presents the results of applying the equations described in the methodology of the mass balance and the values of the experimental properties.

Eq. (11) of the energy balance is then:

$$\dot{m}_{OIL}\left(633.6\left[\frac{kJ}{kg}\right]\right) + 448.43\left[\frac{kJ}{S}\right] = \dot{m}_{OIL}\left(587.25\left[\frac{kJ}{kg}\right]\right) + 1367.24\left[\frac{kJ}{S}\right]$$

Table 4.
Properties of the fluids involved in the system.

Fluid	State	Enthalpy [kJ/kg]	Mass flow rate [kg/s]
Entering thermal oil	Liquid	633.60	-----
Entering fabric	Solid	102.75	8.04 X 10-2
Water entering along with the fabric	Liquid	171.34	3.4503 x 10-2
Air entering Chamber 1	Gas	29.20	2.5872
Air entering Chamber 7	Gas	29.20	2.8728
Water entering along with air into Chamber 1	Gas	1870.00	0.0597
Water entering along with air into Chamber 7	Gas	1870.00	0.0654
Leaving thermal oil	Liquid	587.25	----
Processed fabric	Solid	299.22	8.04 X 10-2
Water leaving along with the fabric	Liquid	506.73	1.7468 X 10-3
Water leaving Extractor fan 1	Gas	2257.00	0.0924
Water leaving Extractor fan 2	Gas	2257.00	0.0654
Evaporated water	Gas	2257.00	3.2756 X 10-2
Air leaving Extractor fan 1	Gas	147.00	2.6217
Air leaving Extractor fan 2	Gas	183.42	2.8728

Source: authors' elaboration

Thus, the mass flow rate of the oil is

$$\dot{\mathrm{m}}_{\mathrm{OIL}} = \frac{918.81\left[\frac{\mathrm{kJ}}{\mathrm{S}}\right]}{46.35\left[\frac{\mathrm{kJ}}{\mathrm{kg}}\right]}$$

$$\dot{\mathrm{m}}_{\mathrm{OIL}} = 19.82\left[\frac{\mathrm{kg}}{\mathrm{S}}\right]$$

The energy flow that enters and leaves along with each fluid in the heat setting process is presented in Table 5.

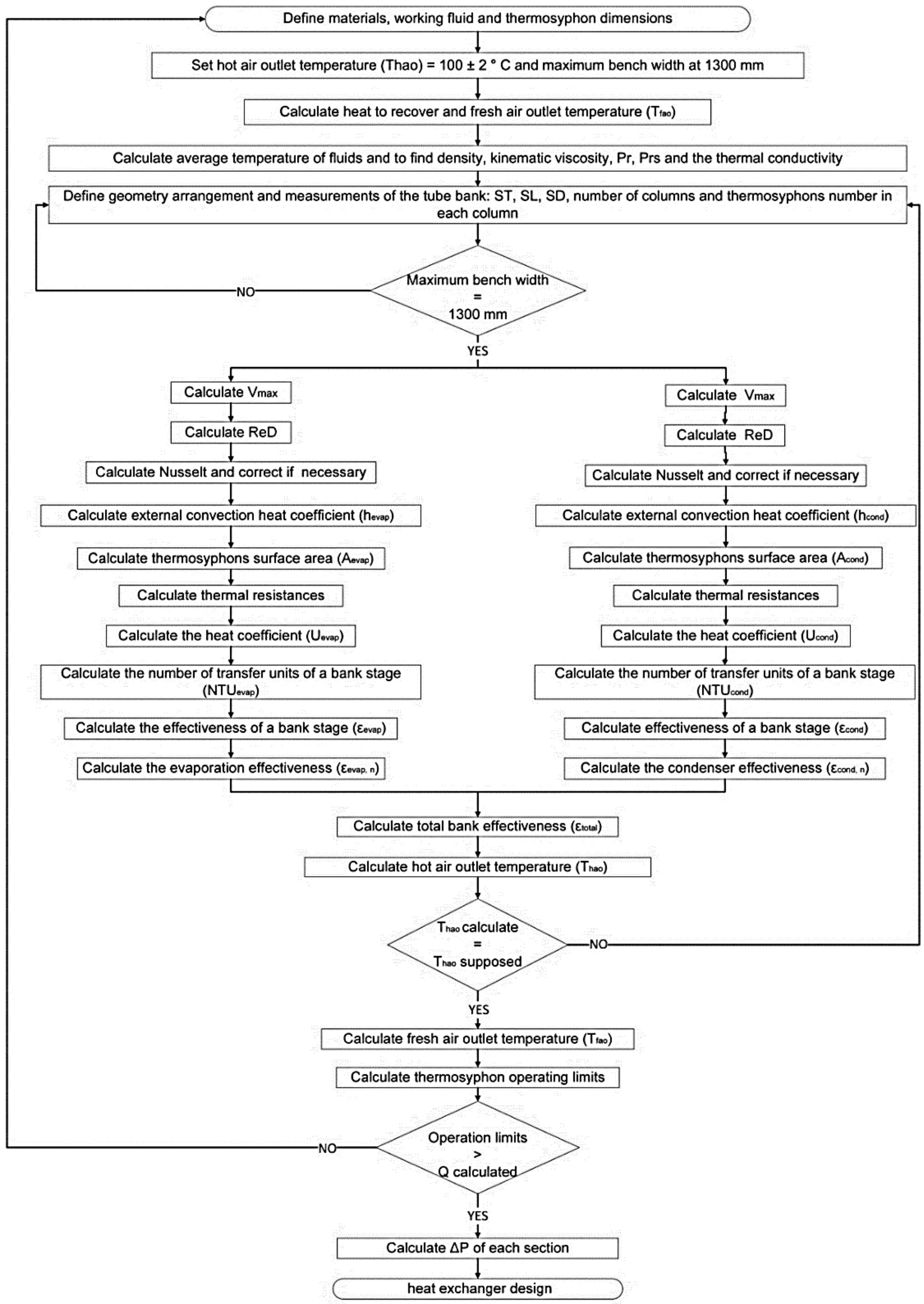

Figure 3. Decision-making map to design the thermosyphon bank.
Source: authors' elaboration.

Table 5.
Energy flows in the heat setting process.

Flow	**Value [kW]**
Energy flow in entering thermal oil	12557.95
Energy flow in entering fabric	8.24
Energy flow in water entering along with the fabric	5.91
Energy flow in air entering Chamber 1	75.54
Energy flow in air entering Chamber 7	83.88
Energy flow in water entering along with air into Chamber 1	110.10
Energy flow in water entering along with air into Chamber 7	122.25
Flow of electrical energy of fans and extractor fans	40.10
Energy flow in leaving thermal oil	11639.29
Energy flow in processed fabric	24.05
Energy flow in water leaving with the fabric	0.88
Energy flow in water leaving Extractor fan 1	132.89
Energy flow in water leaving Extractor fan 2	147.55
Energy flow in evaporated water	73.93
Energy flow in air leaving Extractor fan 1	385.38
Energy flow in air leaving Extractor fan 2	526.92
Energy flow of fans and extractor fans	40.01

Source: authors' elaboration

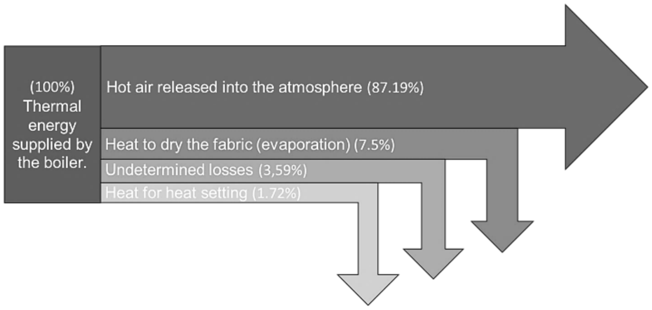

Figure 4. Sankey diagram of the thermal energy used in the stenter.
Source: authors' elaboration

The energy balance shows that the total transferred heat is 918.75 kW, which are supplied by the thermal oil to dry and heat set the fabric, in addition to 40.01 kW of electrical energy that are transformed into work to move the air in the heated chambers and extract it from the stenter. Fig. 4 is a Sankey diagram that represents the thermal energy in this process.

The energy that can be potentially recovered, leaving through the extractor fans of the stenter in the form of hot air, amounts to 800.97 kW, which represents 87.19% of the total energy used in the process. The heat setting process of the fabric selected in this study consumes 11.01 GJ/ton in total, which is 22.00% higher than the maximum values in the literature [5] and may be caused by the age of the equipment and its original design. However, thanks to our analysis, we identified an opportunity to reduce its energy consumption and increase the energy efficiency of the process by recovering heat from the exhaust gases of the stenter to preheat entering air.

3.2 Design of the heat exchanger

Table 6 presents the summary of the results of Heat Exchangers 1 and 2 following the methodology described in Fig. 3. (As the stenter has two extractor fans, the values were calculated for one exchanger per extractor fan.) The table shows a difference in the area of the two exchangers, which is due to the fact that Heat Exchanger 2 has more stages because the fluid enters the equipment at a higher temperature, modifying the convective heat transfer coefficient. Furthermore, thanks to the larger number of stages, its effectiveness is also higher.

Our effectiveness results are in line with those in [21], which reported an effectiveness between 37% and 65%, and [22], in which an effectiveness between 15% and 75% was found. The following section details the configuration and working fluids of the thermosyphons.

3.2.1 Working fluid and material of thermosyphons

The working fluid selected for the thermosyphons was water because the outlet temperatures of the stenter gases are 144.97°C and 180.18°C.

The material of the thermosyphons was Type M copper, which is a kind of economical commercially available tubing in Colombia, where it is mainly used for hot water installations. Furthermore, copper offers high thermal conductivity and is compatible with water.

Table 6.
Results of heat Exchangers 1 and 2.

	Exchanger 1		**Exchanger 2**		
Result	**Evaporator**	**Condenser**	**Evaporator**	**Condenser**	**Unit**
Maximum velocity	12.51	10.23	14.60	11.55	m/s
Reynolds	13026.38	13124.36	12336.55	14084.44	
Nusselt	92.10	93.28	88.62	97.23	
Heat transfer coefficient due to external convection	109.63	93.26	106.41	95.58	W/m² °C
Surface area	45.42	45.42	69.12	69.12	m²
Thermal resistances of the thermosyphons					
	Evaporator	**Condenser**	**Evaporator**	**Condenser**	
By conduction	5.19 x 10-5	5.19 x 10-5	5.19 x 10-5	5.19 x 10-5	°C/W
By convection	1.32 x 10-4	1.51 x 10-4	1.36E-04	1.51 x 10-4	°C/W
By pressure drop	1.07 x 10-8		5.17 x 10-9		°C/W
By boiling	4.16 x 10-6	-----	2.61 x 10-6	-----	°C/W
By condensation	-----	4.04 x 10-3	-----	4.15 x 10-3	°C/W
Total thermosyphon resistance	4.580 x 10-3		4.534 x 10-3		°C/W
Heat transfer coefficient (U)					
	Evaporator	**Condenser**	**Evaporator**	**Condenser**	
Heat transfer coefficient U	109.60	91.69	106.38	93.89	W/m² °C
Effectiveness					
	Evaporator	**Condenser**	**Evaporator**	**Condenser**	
Effectiveness	0.84	0.79	0.92	0.89	
Total effectiveness	0.414		0.459		
Leaving fluid temperatures calculated by NTU					
	80.51		101.56		°C
Hot air	100.97		115.43		°C
Differential pressure and power					
	Evaporator	**Condenser**	**Evaporator**	**Condenser**	
Differential pressure	1619.62	1293.92	3150.16	2437.12	Pa
Power	5.79	3.87	13.13	7.97	kW
Total recovered power					
Total recovered power	118.80		188.03		
Total net power	109.54		166.93		kW

Source: authors' elaboration

Table 7.
Operating temperature of the thermosyphons.

Variable	Value	Unit
Temperature of the gases entering the evaporator in Exchanger 1	144.97	°C
Temperature of the gases entering the evaporator in Exchanger 2	180.18	°C
Temperature of fresh air entering the condenser in both exchangers	35.00	°C
Operating temperature of the thermosyphons in Exchanger 1	90.00	°C
Operating temperature of the thermosyphons in Exchanger 2	107.50	°C
Pressure of saturated water at 90°C [15]	70.14	Kpa
Pressure of saturated water at 107°C [15]	130.68	Kpa

Source: the authors

Table 8.
Characteristics of galvanized steel.

Property	Value
Thickness	1.50 [mm]
Width	1200.00 [mm]
Length	2400.00 [mm]
Weight	33.91 [kg/m]
Creep	230–350 [Mpa]
Strength	310–450 [Mpa]

Source: authors' elaboration

3.2.2 Operating temperature and pressure of the thermosyphons

Table 7 presents the calculated operating temperature and corresponding pressure for saturated water of the thermosyphons in Exchangers 1 and 2.

To ensure the copper tubing would endure the operating pressures, its minimum thickness was

- 0.103 [mm] in Exchanger 1 and
- 0.192 [mm] in Exchanger 2.

These two minimum thicknesses are below that of the copper tubing selected in this study (i.e., 0.889 mm), which can therefore be used ensuring an appropriate operation and minimizing the thermosyphons' risk of breaking.

3.2.3 Casing material

Since the exhaust gases of the stenter contain water vapor, we selected galvanized steel for the casing material. The properties of the latter are presented in Table 8.

3.2.4 Insulation material

The heat exchangers were covered with thermal insulation blankets made of mineral wool, whose properties are detailed in Table 9. The conductivity of this material is low, which is why it is considered adequate for heat exchanger insulation.

3.2.5 Geometric arrangement of the tube bank of the thermosyphons in Exchanger 1

The thermosyphons were placed in a triangular (rotated) staggered configuration with both flows crossing the thermosyphons. Such geometric array was selected so that the (hot or fresh) air comes into contact with the thermosyphons in its way in the second row, thus avoiding possible outlet ways without maximum contact with the thermosyphons.

Table 10 details the initial values that were randomly assumed and the final values after the iterative process was completed following the decision-making map.

Table 9.
Characteristics of the thermal insulation blanket.

Property	Value
Density	140.000 [km/m³]
Thermal conductivity at 200°C	0.055 [W/ m K]
Maximum service temperature	1023.150 [K]

Source: authors' elaboration

Table 10.
Measurements of the thermosyphon bank in Exchanger 1 and constraints.

Variable	Initial value	Final value	Units
Cross pitch (ST)	35	54.57	mm
Diagonal pitch (DS)	39.13	42.05	mm
Longitudinal pitch (SL)	35	32	mm
Condenser length (LC)	200	500	mm
Evaporator length (LE)	200	500	mm
Adiabatic region length (LA)	0	0	mm
Total thermosyphon length (LTT)	400	1000	mm
Number of columns	40	22	Number
Number of rows	40	46	Number
Outlet temperature of fresh air	60	80.54	°C
Outlet temperature of hot air	116	100.77	°C
Thermosyphon bank width	2171	1255	mm

Source: authors' elaboration

3.2.6 Equivalent thermal conductivity of a thermosyphon

Finally, the total thermal resistance and conductivity of a thermosyphon are, respectively,

$$R_{Total} = 4.58 \times 10^{-3} \left[\frac{°C}{W}\right]$$

$$K = 340511.82 \left[\frac{W}{m^2.K}\right]$$

This conductivity, a result of the total thermal resistance that was found, is 851 higher than that of copper (average copper conductivity: 400 W/m²°C). Zohuri (2016) described a thermosyphon, with water as working fluid, that has an effective thermal conductivity in the order of 1x105 W/m²°C; in addition, depending on design and operating conditions, it is common to find values around 4x105, which is 1000 times higher than that of copper. Other studies [20,23,24] support this result and associate it with high heat transfer coefficients in boiling and condensation processes.

3.2.7 Operating limits of the thermosiphon

Table 11 presents the operating limits obtained for the thermosyphon designed here. The volume of liquid used to calculate the dry-out limit was 50% of the evaporator, which

Table 11.
Operating limits of the thermosyphons in Exchanger 1.

Limit	Value	Unit
Dry-out limit	97796097.85	W
Sonic limit	107684.2558	W
Entrainment limit	9410.308531	W
Viscous limit	Not applicable	
Boiling limit	37983.26989	W

Source: authors' elaboration

Table 12.
Parameters to calculate the differential pressure.

Parameter	Value
ST/D	1.91
ST/SL	1.3
f friction factor	0.6
X factor	1

Source: authors' elaboration

is a volume of 0.000140679 m3 of water. Considering that Exchanger 1 is composed of 1012 thermosyphons, which are subjected to a heat flow of 118802 W, and if each thermosyphon transfers the same amount of energy, as a result, we have that each thermosyphon will be subjected to a maximum heat flow of 117.4 W. This value is significantly lower than those found for each one of the operating limits, which indicates that the design proposed here is adequate.

It can be concluded that the thermosyphons operate without a problem because the maximum heat flow is never above any of their operating limits.

3.2.8 Mechanical design

The parameters to calculate the differential pressure are presented in Table 12:

The differential pressures for the evaporation and condensation sections are

$$\Delta P_{evap} = 1619.62\ [Pa]$$
$$\Delta P_{evap} = 1293.92\ [Pa]$$

The power needed to move the hot and fresh air through Exchanger 1 is

$$\dot{W}_{Hot\ fan} = 5.79[kW]$$
$$\dot{W}_{Fresh\ fan} = 3.87[kW]$$

This additional power needed to install the heat exchange system represents 8.16% of the total power recovered with Exchanger 1 and 11.2% of that with Exchanger 2. These values are low considering the global size of the equipment.

4. Conclusions

We found that, in the process of fabric drying and heat setting in a stenter, the main heat transfer occurs in the heated chambers. The mass and energy balances showed that the thermal consumption of the stenter amounted to 918.65 kW, 95.82% of which are supplied as thermal energy by the hot thermal oil and 4.18% as electricity. Out of the total thermal energy, 800.97 kW are available in the hot air used in the process.

The heat setting process of the stenter analyzed in this study consumes 11.01 GJ/ton in total, which is 22% higher than the maximum values in the literature and may represent an opportunity for improving its energy efficiency. Finally, using this heat recovery system with thermosyphons, the thermal energy consumption of the stenter can be reduced by 30.1%.

References

[1] BSC INCORPORATED, Waste heat recovery: technology opportunities in the US industry, Waste Heat Recover. Technol. Oppor. US Ind., 2008, pp. 1-112. DOI: 10.1017/CBO9781107415324.004.

[2] The European Commission, Integrated pollution prevention and control (IPPC). Reference document on best available techniques for the textiles industry, July, 2003, 626 P.

[3] Rakib, M.I., Saidur, R., Mohamad, E.N. and Afifi, A.M., Waste-heat utilization - The sustainable technologies to minimize energy consumption in Bangladesh textile sector, J. Clean. Prod., 142, pp. 1867-1876, 2016. DOI: 10.1016/j.jclepro.2016.11.098.

[4] Aranda-Usón, A., Ferreira, G., Mainar-Toledo, M.D., Scarpellini, S. and Llera-Sastresa, E., Energy consumption analysis of Spanish food and drink, textile, chemical and non-metallic mineral products sectors, Energy, 42(1), pp. 477-485, 2012. DOI: 10.1016/j.energy.2012.03.021.

[5] Schönberger, H. and Schäfer, T., Best Available techniques in textile industry, 2003, 364 P.

[6] Hasanbeigi, A., Energy-efficiency improvement opportunities for the textile industry, Lawrence Berkeley Natl. Lab., 2010, 136 P.

[7] Elahee, K., Heat recovery in the textile dyeing and finishing industry: lessons from developing economies, 21(3), pp. 9-15, 2010.

[8] Tian, E., He, Y.L. and Tao, W.Q., Research on a new type waste heat recovery gravity heat pipe exchanger, Appl. Energy, 188, pp. 586-594, 2017. DOI: 10.1016/j.apenergy.2016.12.029.

[9] Cay, A., Tarakçioğlu, I. and Hepbasli, A., Exergetic performance assessment of a stenter system in a textile finishing mill, Int. J. Energy Res., 31(August) pp. 1251-1265, 2007. DOI: 10.1016/j.apenergy.2016.12.029.

[10] Cay, A., Tarakçioğlu, I. and Hepbasli, A., A study on the exergetic analysis of continuous textile dryers, Int. J. Exergy, 6(3), pp. 422-439, 2009. DOI: 10.1504/IJEX.2009.025348.

[11] Cay, A., Tarakçioğlu, I. and Hepbasli, A., Exergetic analysis of textile convective drying with stenters by subsystem models: Part 1-exergetic modeling and evaluation, Dry. Technol., 28(12), pp. 1359-1367, 2010. DOI: 10.1080/07373937.2010.482695.

[12] Quispe, B., Recomendaciones para calibración y uso de termómetros de radiación infrerroja, 2013.

[13] IDEAM, Método 1 determinación del punto y velocidad de muestreo para fuentes estacionarias, No. 2, pp. 1-22, 2011.

[14] PSICRO, [Online]. 2008. Available at: http://www.psicro.org/psicro/psicrocalc.html. [Accessed: 11-Oct-2019].

[15] Cengel, Y.A., Transferencia de calor y masa, Biotechnol. Lett., 18(12), pp. 1419-1422, 2007. DOI: 10.1007/BF00129346.

[16] Faghri, A. and Ang, Y., Transport phenomena in multiphase systems. 2006.

[17] Mroue, H., Ramos, J.B., Wrobel, L.C. and Jouhara, H., Performance evaluation of a multi-pass air-to-water thermosyphon-based heat exchanger, Energy, 139, pp. 1243-1260, 2017. DOI: 10.1016/j.energy.2017.04.111.

[18] Mroue, H., Ramos, J.B., Wrobel, L.C. and Jouhara, H., Experimental and numerical investigation of an air-to-water heat pipe-based heat exchanger, Appl. Therm. Eng., 78, pp. 339-350, 2015. DOI: 10.1016/j.applthermaleng.2015.01.005.

[19] Ramos, J., Chong, A. and Jouhara, H., Experimental and numerical investigation of a cross flow air-to-water heat pipe-based heat exchanger used in waste heat recovery, Int. J. Heat Mass Transf., 102, pp. 1267-1281, 2016. DOI: 10.1016/j.ijheatmasstransfer.2016.06.100.

[20] Reay, D.A., Kew, P.A. and McGlen, R.J., Heat Pipes, 2014.
[21] Noie, S.H., Investigation of thermal performance of an air-to-air thermosyphon heat exchanger using ε-NTU method, Appl. Therm. Eng., 26(5-6), pp. 559-567, 2006. DOI: 10.1016/j.ijheatmasstransfer.2016.06.100.
[22] Danielewicz, J., Sayegh, M.A., Śniechowska, B., Szulgowska-Zgrzywa, M. and Jouhara, H., Experimental and analytical performance investigation of air to air two phase closed thermosyphon based heat exchangers, Energy, 77, pp. 82-87, 2014. DOI: 10.1016/j.energy.2014.04.107.
[23] Zohuri, B., Heat pipe design and technology: modern applications for practical thermal management, 2nd ed., 2016.
[24] Vasiliev, L. and Kakac, S., Heat pipes and solid sorption transformations: fundamentals and practical applications, Routledge, Taylor & Francis Group, UK, 2014, 536 P.

R. Mazo-Restrepo, received the BSc. Eng in Electrical Engineering in 2013, from the Universidad de Antioquia, Medellín, Colombia, the MSc. in Industrial Energy Management in 2020, it is finished and awaiting degrees from the Instituto Tecnológico Metropolitano in Medellín, Colombia. From 2010 to 2021 he has worked in the textile industry where he has developed energy use projects. His research interests include: simulation of thermal systems, heat transfer and combustion, energy audits, renewable energy and heat transfer systems.
ORCID: 0000-0002-5132-8810

P.N. Alvarado, is BSc. in Chemistry and received his PhD. Sc. in Chemistry in 2017, from the Universidad de Antioquia, Colombia. He is currently a professor of the Instituto Tecnológico Metropolitano (ITM), in Medellín.
ORCID: 0000-0002-4435-3989

K. Cacua, received the BSc. Eng. in Chemical Engineering in 2006, from the Universidad Industrial de Santander, Bucaramanga, Colombia, the MSc. in Engineering in 2010, from the Universidad de Antioquia, Medellin, Colombia, and the PhD in Engineering Science and Technology of Materials in 2019, from the Universidad Nacional de Colombia, Medellin, Colombia. From 2011 to 2021, she has been worked for Instituto Tecnológico Metropolitano in Medellín, Colombia. Currently, she is a professor in the Electromechanics and Mecatronics Department, Facultad de Ingenierías, Instituto Tecnológico Metropolitano. Her research interests include: nanofluids for heat transfer and combustion, engines, thermal systems simulation, energy audits, renewable energies and heat transfer systems.
ORCID: 0000-0001-7535-9622